PHYSICAL REVIEW D **86,** 033003 (2012)

Constraints on new scalars from the LHC 125 GeV Higgs signal

We-Fu Chang*

Department of Physics, National Tsing Hua University, and Physics Division, National Center for Theoretical Sciences, No. 101, Section 2, Kuang-Fu Road, Hsinchu, Taiwan 30013, Republic of China

John N. Ng†

TRIUMF, 4004 Wesbrook Mall, Vancouver, British Columbia, V6T 2A3, Canada

Jackson M. S. Wu‡

Physics Division, National Center for Theoretical Sciences, No. 101, Section 2, Kuang-Fu Road, Hsinchu, Taiwan 30013, Republic of China

(Received 1 July 2012; published 3 August 2012)

We study the implications the recent results from the LHC Higgs searches have on scalar new physics. We study the impact on both the Higgs production and decay from scalars with and without color, and in cases where decoupling does and does not happen. We investigate possible constraints on scalar parameters from the production rate in the diphoton channel, and also the two vector boson channels. Measurements from both channels can help disentangle new physics due to color from that due to charge, and thus reveal the nature of the new scalar states.

DOI: 10.1103/PhysRevD.86.033003 PACS numbers: 14.80.Bn, 13.85.Qk, 14.80.Ec, 14.80.Fd

I. INTRODUCTION

A central piece of the Large Hadron Collider (LHC) program is to find the standard model (SM) Higgs boson, or else discover scalar particle(s) of similar properties. The LHC has great sensitivity for Higgs produced via gluon fusion, which then decays into electroweak gauge bosons. So far, no significant excess of events has been seen in the mass range of 129 GeV to 600 GeV at 95% confidence level [1]. But at around 125 GeV, both the ATLAS [2] and CMS [3] detectors observed an excess at the 3σ level in the diphoton channel. The ATLAS collaboration also reported an excess in the ZZ^* channel in this mass range [4], although the CMS search in this channel yielded a less significant result [5]. Taken at face value, the recent LHC data seem to suggest a central value of the diphoton production rate 1.5 to 2 times the SM value, but one consistent with the SM for the ZZ^* production. There were also Higgs searches at the Tevatron, which is sensitive for a Higgs mass below 200 GeV. A broad excess interpretable as a SM Higgs decaying into a pair of bottom quarks was observed [6]. The statistical significance is not sufficient to claim discovery. Nevertheless, it is tantalizing. The current run at the LHC will certainly clarify the situation.

The unexpected enhancement in the diphoton production rate has motivated many recent studies on possible new physics (NP) explanations (see e.g. [7] and references within). The diphoton channel is a very clean channel that is sensitive to corrections in both the production cross section and the decay width. New scalar states have been widely considered as possible sources. A lot of studies have investigated in specific models their impact on either the Higgs production via gluon-gluon fusion (GF), which is the dominant production process, or the Higgs decay in the diphoton channel. Here, we study the generic effect the new scalars have on both the Higgs production and decay. Besides the GF production and the diphoton decay, we also include in our study the productions from vector boson fusion (VBF) and associate production with vector boson (VH), $V = W, Z$, and decay into two vector bosons. We emphasize that by measuring the production rates in different decay channels, or in the same decay channel but from different production processes, information about the color and the charge of the new scalar states can be obtained.[1]

A feature we pay close attention to is whether the effects of the new scalar states decouple as they become heavy. In general, colored scalars are naturally of the decoupling type as their masses do not share the same origin as the SM Higgs. On the other hand, scalars that mix with the SM Higgs tend not to decouple. Properties of the new scalar state may be revealed from this perspective. This has not been emphasized before, and it could be a useful tool for indirect searches of NP.

This paper is organized as follows. In Sec. II we discuss in general how NP can modify the LHC Higgs signal. In Sec. III we study classes of scalar NP according to their $SU(3)$ color and $SU(2)$ weak representations using explicit examples, and we investigate the constraints from

*wfchang@phys.nthu.edu.tw
†misery@triumf.ca
‡jknw350@yahoo.com

[1]Currently, the associate production cannot be separated out from GF and other production mechanisms. However, we anticipate this to be feasible in the future LHC runs with high energy and high luminosity.

production rates in the $\gamma\gamma$ and VV^* channel. Section IV contains our conclusions.

II. GENERAL CONSIDERATIONS

At the LHC, the Higgs boson is produced predominantly through GF. To a lesser degree production also proceeds through VBF: VH processes can also be non-negligible if the Higgs is light. For the decay, we focus mainly on the diphoton and the VV^* channels for which the LHC is sensitive. In the SM, both the GF production of the Higgs and its diphoton decay start at the one-loop level, while VBF, VH, and $H \to VV^*$ are all processes that start at the tree level. Most NP scenarios do not alter the tree-level processes. An exception is when there is large admixture of new spin-0 states with the SM Higgs, or new spin-1 states with the SM gauge bosons. Since no new vector bosons were found, it is reasonable to assume that the as yet undiscovered spin-1 states have small mixing with the SM gauge bosons. The question of the Higgs mixing with new scalar or pseudoscalar states is however open. In general, such mixing will reduce the strength of the Higgs couplings to W and Z with respect to their SM values. The Higgs couplings to fermions are likely to be similarly affected which, in particular, would have consequences for $H \to b\bar{b}$, the dominant decay mode for a light 125 GeV Higgs. In later sections we study the effects of scalar mixings with explicit examples.

We focus here on how NP affect the loop-induced processes: $gg \to H$ and $H \to \gamma\gamma$. To have our analysis as model-independent as possible, we base our study on the spin, masses and couplings of the NP. We discuss the generalities of NP effects from spin-0 and spin-1/2 new states below. We leave the investigation of higher spin NP for future works.

In order to affect the GF process, the new degrees of freedom must couple to the Higgs and have nontrivial color $SU(3)$ representations. Similarly, to affect the diphoton decay they must be electrically charged. Thus new neutrino states, sterile or otherwise, have no bearing in our consideration. We note that since the NP would interfere with SM processes at the amplitude level, it is not surprising that, if confirmed, the LHC signal can severely restrict the possible couplings of these new degrees of freedoms with the SM Higgs.

Consider first the Higgs diphoton decay. Including spin-0 and spin-1/2 NP contributions, the width is given by

$$\begin{aligned}\Gamma_{\gamma\gamma} &\equiv \Gamma(H \to \gamma\gamma) \\ &= \frac{G_\mu \alpha^2 M_H^3}{128\sqrt{2}\pi^3} \Big| F_1(\tau_W) + \frac{4}{3} F_{1/2}(\tau_t) \\ &\quad + \sum_\phi d(r_\phi) Q_\phi^2 \frac{\lambda_\phi}{g_w} \frac{M_W^2}{M_\phi^2} F_0(\tau_\phi) \\ &\quad + \sum_f d(r_f) Q_f^2 \frac{2y_f}{g_w} \frac{M_W}{M_f} F_{1/2}(\tau_f) \Big|^2, \end{aligned} \tag{1}$$

where G_μ is the Fermi constant, α the fine structure constant, and g_w the weak gauge coupling. The first two terms are the SM one-loop contributions from the W and the top quark. It is well known that the W loop dominates in the SM and the top contribution subtracts from it. Following the conventions of Ref. [8], we define $\tau_i \equiv M_H^2/(4M_i^2)$, and the one-loop functions are given by

$$\begin{aligned} F_0(\tau) &= -[\tau - f(\tau)]\tau^{-2}, \\ F_{1/2}(\tau) &= 2[\tau + (\tau - 1)f(\tau)]\tau^{-2}, \\ F_1(\tau) &= -[2\tau^2 + 3\tau + 3(2\tau - 1)f(\tau)]\tau^{-2}, \end{aligned} \tag{2}$$

with

$$f(\tau) = \begin{cases} \arcsin^2\sqrt{\tau} & \tau \le 1 \\ -\frac{1}{4}\left[\log\frac{1+\sqrt{1-\tau^{-1}}}{1-\sqrt{1-\tau^{-1}}} - i\pi\right]^2 & \tau > 1. \end{cases} \tag{3}$$

In NP contributions, we see explicitly the dependence on Q, the electric charge of the new particle. The color dependence enters through $d(r)$, the dimension of the color representation r of the new particle. Unlike the Yukawa coupling y_f of the Higgs to new fermions, the $H\phi\phi$ coupling is dimensionful. For convenience we scale it using the W boson mass so that it is $\lambda_\phi M_W$. In general the phases of y_f and λ_ϕ relative to g_w are not determined. However, they can be fixed in specific models.

For the GF production, the parton level cross section can be written as

$$\sigma_{gg} \equiv \hat{\sigma}(gg \to H) = \sigma_0 M_H^2 \delta(\hat{s} - M_H^2), \tag{4}$$

where

$$\begin{aligned}\sigma_0 = \frac{G_\mu \alpha_s^2}{128\sqrt{2}\pi} \Big| &\frac{1}{2} F_{1/2}(\tau_t) + \sum_\phi \frac{\lambda_\phi}{g_w} \frac{M_W^2}{M_\phi^2} C(r_\phi) F_0(\tau_\phi) \\ &+ \sum_f \frac{2y_f}{g_w} \frac{M_W}{M_f} C(r_f) F_{1/2}(\tau_f) \Big|^2. \end{aligned} \tag{5}$$

The first term is the SM contribution dominated by the top loop. The color dependence in the NP contributions enters here through $C(r)$, the index of the representation r.[2]

Comparing Eqs. (1) and (5), we see similar NP contributions to both the GF production and the diphoton decay. The differences are in the color factors and electric charges. Partial compensation of NP contributions are thus expected when considering the event rates from the reaction chain $gg \to H \to \gamma\gamma$. This has been noted previously in the study of models with fourth generation fermions.

From Eqs. (1) and (5), we see also that NP contributions scale as M_ϕ^{-2} for scalars and M_F^{-1} for fermions for large masses. This follows from the fact that in the large mass limit

[2]For a particle in the $SU(3)$ representation r with generator T_r^a, $\mathrm{Tr} T_r^a T_r^b = C(r)\delta^{ab}$. Normalizing such that $C(\mathbf{3}) = 1/2$, we have $C(\mathbf{6}) = 5/2$ and $C(\mathbf{8}) = 3$.

$$F_0(\tau) \underset{r\to 0}{\to} \frac{1}{3}, \qquad F_{1/2}(\tau) \underset{r\to 0}{\to} \frac{4}{3}. \tag{6}$$

It may appear at first sight that NP would always decouple as new particles become heavy. However, this is not necessarily the case in general: decoupling would not happen if the effective couplings λ_ϕ and y_f also scale as the mass. This is illustrated for example by fourth generation models with a SM Higgs doublet, where Yukawa couplings $y_f \sim M_F/M_W$. The mass dependence resides in $F_{1/2}(\tau)$, which approaches a constant. The nondecoupling effect leads to the well known demise of the model as noted in [9]. The LHC Higgs search in channels considered above are particularly sensitive for this class of models.

In the following we specialize to scalar NP. We pay particular attention to cases where nondecoupling occurs. All our analyses below are performed for the case of LHC at $\sqrt{s} = 8$ TeV.

III. SCALAR NEW PHYSICS

A. Scalars with color: General features

If a scalar field ϕ carries color, its mass cannot be the result of spontaneous symmetry breaking (SSB): a colored vacuum would result otherwise. Prominent classes of examples are squarks in supersymmetric models, scalar leptoquarks that couple to quarks and leptons, and fermiophobic colored scalars. The squark masses arise mainly from soft breaking mass and can be taken to infinity independent of electroweak symmetry breaking. Similarly, masses of the leptoquark and colored scalar are free parameters in the effective theory at or near the electroweak scale. The only relevant coupling is the $H\phi^\dagger\phi$ coupling, which can arise from the gauge invariant interaction term

$$\lambda_\phi \phi^\dagger \phi H^\dagger H \overset{\text{SSB}}{\to} \lambda_\phi \frac{v}{\sqrt{2}} \phi^\dagger \phi H, \tag{7}$$

where $v = 246$ GeV sets the Fermi scale, and SSB contributes an amount $\lambda_\phi v^2/2$ to the mass of the scalar, M_ϕ^2. The effective coupling λ_ϕ is independent of M_ϕ, and such scalars are of the decoupling type. The sign of λ_ϕ is not fixed *a priori* and is model-dependent. Colored scalars can contribute to either or both GF production and the diphoton decay. VBF and VH productions are not affected.

We illustrate in Figs. 1 and 2 how the GF production cross section and the diphoton decay width of the Higgs are changed with respect to the SM by the colored scalar NP. The decoupling nature of the colored scalar is evident. It sets in at $M_\phi \sim 1$ Tev for the range of coupling we consider. Comparing the two figures, we see also how the partial compensation of NP effects can happen from production to decay. Noting that the current data have very low statistics, we use the expected SM values as a guide for constraints on the NP parameter space. Specifically, we take the theoretical 1σ uncertainty in the SM normalization used as a benchmark. Here, the theoretical 1σ uncertainty in σ_{gg}^{SM} is $\pm 14.7\%$, and in $\Gamma_{\gamma\gamma}^{\text{SM}}$ $[-6.3\%, 6.4\%]$ [10].

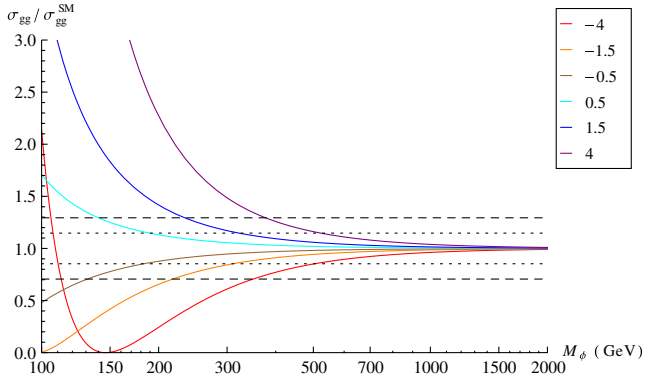

FIG. 1 (color online). The SM normalized Higgs production cross section via GF for various values of $\lambda_\phi C(r_\phi)$ as denoted by the colored lines. [From top to bottom, the lines correspond to $\lambda_\phi C(r_\phi) = 4$ to -4.] The dotted (dashed) lines give bounds from the theoretical 1σ (2σ) uncertainty in the determination of σ_{gg}^{SM}.

As can be seen from Eqs. (1) and (5), for λ_ϕ sufficiently negative, there can be a cancellation between the SM top and the scalar NP contributions. Moreover, for M_ϕ sufficiently light, the scalar NP contribution can become large and completely dominate over that from the SM top. Such behavior is seen in Fig. 1 in the case of $\lambda C(r_\phi) = -4$, where $\sigma_{gg} = 0$ at $M_\phi = 146.1$ GeV [for $\lambda C(r_\phi) = -1.5$, the zero occurs at $M_S = 97.0$ GeV].

Recent LHC data suggest that $R_{\gamma\gamma} \sim 1.5$ to 2 [2,3], where $R_{\gamma\gamma}$ is the ratio of the diphoton production rates defined by

$$R_{\gamma\gamma} = \frac{\sigma(pp \to H + X)\text{Br}(H \to \gamma\gamma)}{\sigma_{\text{SM}}(pp \to H + X)\text{Br}_{\text{SM}}(H \to \gamma\gamma)}. \tag{8}$$

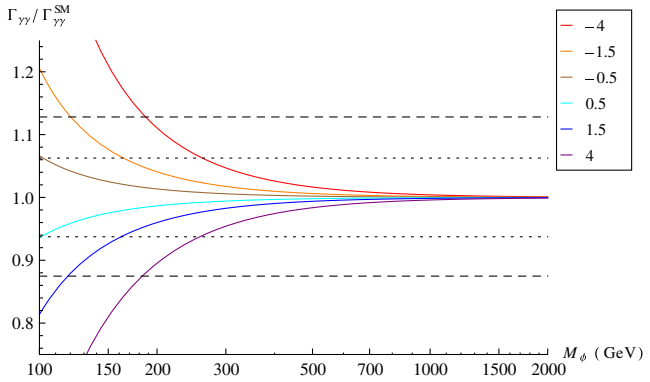

FIG. 2 (color online). The SM normalized Higgs diphoton decay width for various values of $\lambda_\phi d(r_\phi) Q_\phi^2$ as denoted by the colored lines. [From top to bottom, the lines correspond to $\lambda_\phi d(r_\phi) Q_\phi^2 = -4$ to 4.] The dotted (dashed) lines give bounds from the theoretical 1σ (2σ) uncertainty in the determination of $\Gamma_{\gamma\gamma}^{\text{SM}}$.

Given that GF is the dominant Higgs production mechanism at the LHC (about 88% of the total cross section [10]), and that the branching ratio is not expected to be wildly different from the SM for most mass ranges (cf. Fig. 2), such enhancement should be reflected in the ratio $\sigma_{gg}/\sigma_{gg}^{\rm SM}$. Figure 1 would then suggest that having λ_ϕ negative [$C(r_\phi)$ is positive] is unlikely to give rise to the purported enhancement, unless its magnitude is large. However, the allowed range for M_ϕ is then much smaller than for the corresponding postil valued coupling. This is again illustrated by the $\lambda C(r_\phi) = -4$ case.

Although Higgs production cross sections and decay widths (or branching ratios) are not separately measured at the LHC, information pertaining to the color and the charge of the new scalar states can be extracted by simultaneously measuring both $R_{\gamma\gamma}$ and R_{VV}, a quantity similarly defined but for the $H \to VV^*$ channel. This is so because the two have parametrically different dependences on $d(r_\phi)Q_\phi^2$ in the branching ratios.

Such a procedure can be made even sharper if the VH production cross section can be measured on its own, separate from that of the GF, which is the only production mechanism affected by the color of the NP. This is anticipated to be possible at 14 TeV with high luminosity and high statistics. By measuring also

$$R_{\gamma\gamma}^{VH} = \frac{\sigma(pp \to VH)\mathrm{Br}(H \to \gamma\gamma)}{\sigma_{\rm SM}(pp \to VH)\mathrm{Br}_{\rm SM}(H \to \gamma\gamma)}, \qquad (9)$$

complementary information on the color representation can be extracted, which can then be used to extract information about the charge Q_ϕ.

Below we study in detail the role of the electric charge in colored scalars.

1. Electrically neutral colored scalars: $Q_\phi = 0$

By being electrically neutral, these colored scalars contribute only to the GF process. The GF production cross section can be altered significantly for large color representations. All other Higgs production channels and the diphoton decay are unchanged from the SM.

We show in Fig. 3 the ratio $R_{\gamma\gamma}$ as a function of M_ϕ, the mass of the colored scalar particle, for various values of $\lambda_\phi C(r_\phi)$. The theoretical 1σ uncertainty in the SM diphoton production rate is $\pm 13.8\%$. In making the plot and deriving the uncertainties, we have used values of SM Higgs production cross sections and branching ratios compiled in Ref. [10].

Note for $Q_\phi = 0$, $R_{VV} = R_{\gamma\gamma}$. This is an important prediction for this class of scalar NP. Preliminary data suggest that the two are not equal [1]. If this finding persists, it would rule out the electrically neutral colored scalars as the source of deviation from the SM.

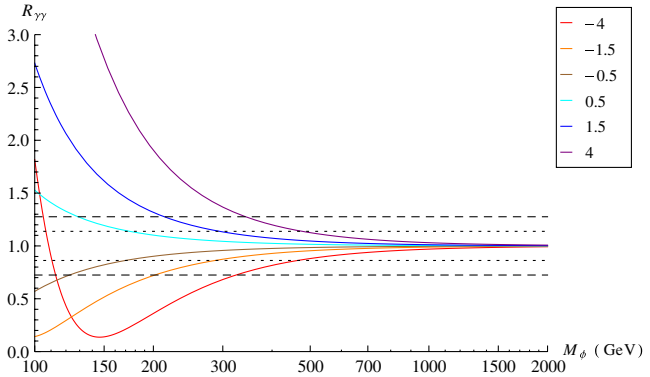

FIG. 3 (color online). The SM normalized production rate $R_{\gamma\gamma}$ for the case of charge neutral scalar NP. The colored lines denote various values of $\lambda_\phi C(r_\phi)$. [From top to bottom, the lines correspond to $\lambda_\phi C(r_\phi) = 4$ to -4.] The dotted (dashed) lines give bounds from the total theoretical 1σ (2σ) uncertainties in the SM diphoton production rate.

2. Electrically charged colored scalars: $Q_\phi \neq 0$

With electric charge, the colored scalars modify both the GF production cross section and the diphoton decay width. In Fig. 4 we show how $R_{\gamma\gamma}$ depends on $\lambda_\phi C(r_\phi)$ and $\lambda_\phi d(r_\phi)Q_\phi^2$. We see for the mass range we consider, an enhancement in $R_{\gamma\gamma}$ would require in general a positive λ_ϕ.[3] Enhancement for negative λ_ϕ is possible, but happens only for $|\lambda_\phi C(r_\phi)|$ sufficiently large, and in a much more restrictive mass range in the low mass region. In fact, the lower the mass, the larger the enhancement. This is a general trend seen in Figs. 1 and 3. The new feature here is that the smaller the ratio $d(r_\phi)Q_\phi^2/C(r_\phi)$, the larger the enhancement. This is because for fixed λ_ϕ and $C(r_\phi)$, increasing $d(r_\phi)Q_\phi^2$ depresses the diphoton width as is seen in Fig. 2. Note that the variation due to $d(r_\phi)Q_\phi^2$ is smaller when λ_ϕ is negative.

Since the $H \to VV^*$ width is unchanged from the SM, and the contribution of $\Gamma_{\gamma\gamma}$ to the total width is very small, R_{VV} is just $R_{\gamma\gamma}$ in the $Q_\phi = 0$ case plotted in Fig. 3. A difference between R_{VV} and $R_{\gamma\gamma}$ would favor the interpretation that colored scalars are electrically charged. Comparing Figs. 3 and 4, this appears to be the case in general.

Another useful diagnostic here is $R_{\gamma\gamma}^{VH}$, which we show in Fig. 5. The total theoretical 1σ uncertainty in the SM diphoton rate from VH production (the total from both WW and ZZ) is $\pm 5.8\%$. Note that $R_{\gamma\gamma}^{VH}$ is just $\mathrm{Br}(H \to \gamma\gamma)$ normalized to the SM since the VH production is unchanged from the SM. Hence we see enhancement (suppression) for negative (positive) values of $\lambda_\phi C(r_\phi)$, like $\Gamma_{\gamma\gamma}/\Gamma_{\gamma\gamma}^{\rm SM}$ seen in Fig. 2. Comparing $R_{\gamma\gamma}^{VH}$ with $R_{\gamma\gamma}$ would allow the contribution from colored NP in σ_{gg} to be extracted.

[3] $C(r_\phi)$, $d(r_\phi)$, and Q^2 are all positive quantities

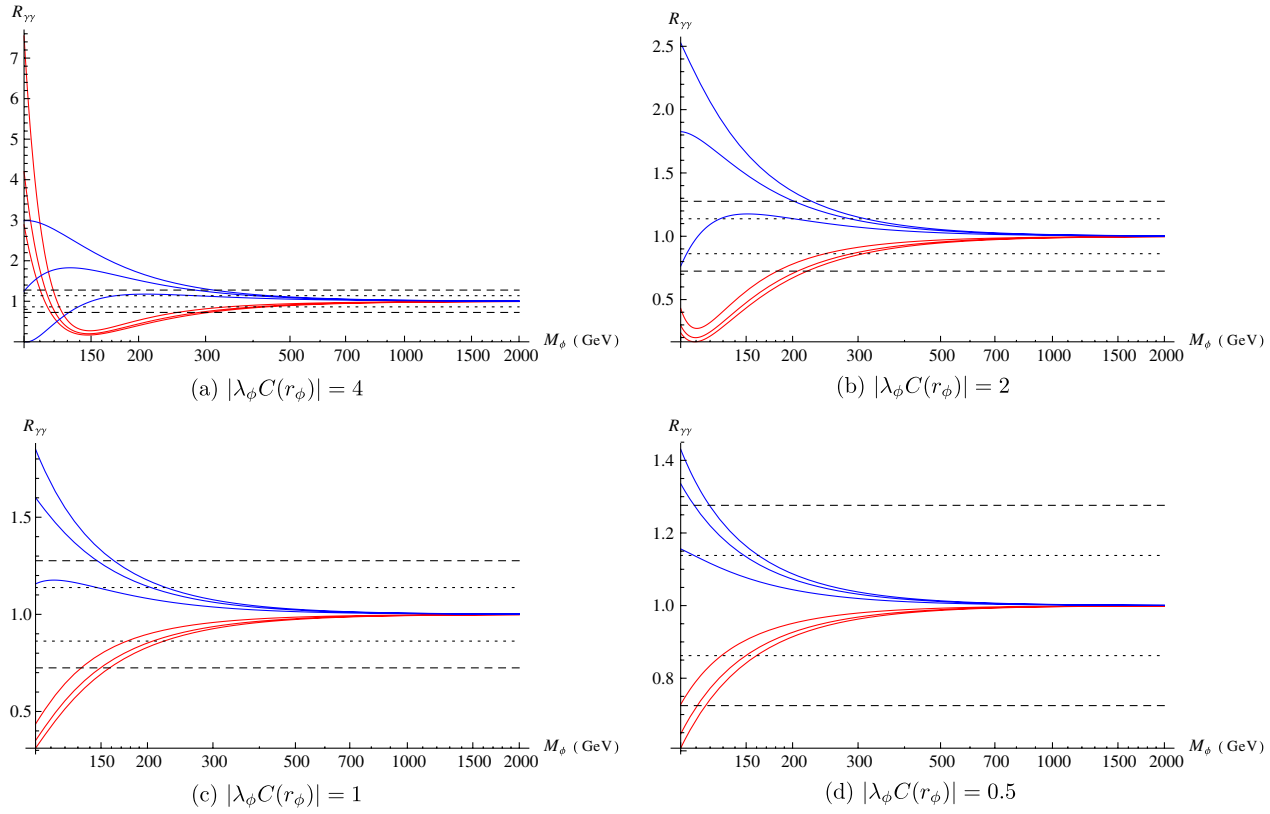

FIG. 4 (color online). The SM normalized production rate $R_{\gamma\gamma}$ for the case of charged scalar NP for various values of $\lambda_\phi C(r_\phi)$ and $\lambda_\phi d(r_\phi) Q_\phi^2$. The blue (red, the lower three at large M_ϕ) lines correspond to positive (negative) values of $\lambda_\phi C(r_\phi)$. From top to bottom, the blue lines correspond to $d(r_\phi)Q_\phi^2/C(r_\phi) = 1, 2, 4$. For red lines, this ordering is reversed. The dotted (dashed) lines give bounds from the total theoretical 1σ (2σ) uncertainties in the SM diphoton production rate.

B. Scalars without color

Models of color singlet scalars are very well studied for various phenomenological motivations ranging from neutrino mass generation to flavor physics: it is also an integral part of the minimal supersymmetric SM. We are interested here primarily in how the 125 GeV Higgs signal at the LHC is relevant in these models. The most important aspect for us is then the scalar potential. We organize our study by classifying the scalars according to their $SU(2)$ representation. Below we investigate in detail cases of singlet,

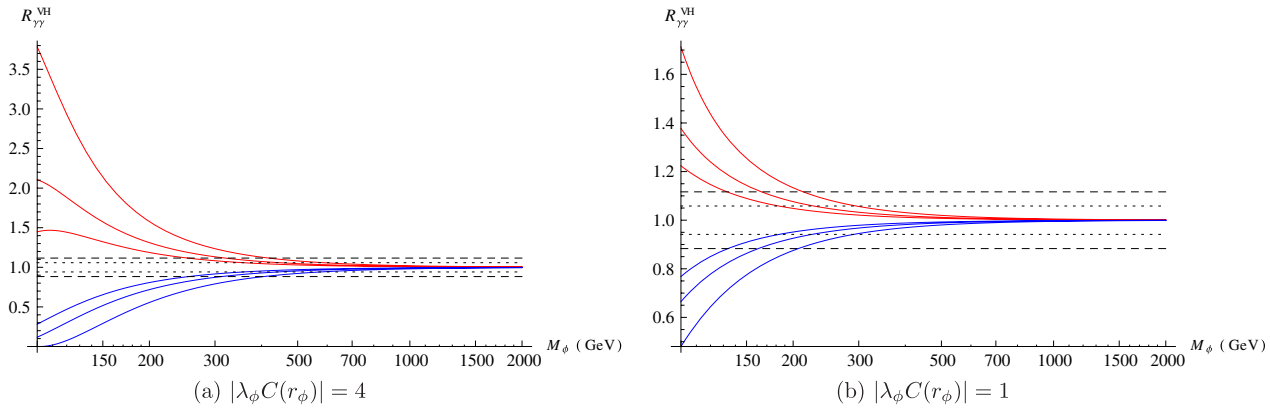

FIG. 5 (color online). The SM normalized production rate $R_{\gamma\gamma}^{VH}$ for various values of $\lambda_\phi C(r_\phi)$ and $\lambda_\phi d(r_\phi) Q_\phi^2$. The blue (red, the upper three) lines correspond to positive (negative) values of $\lambda_\phi C(r_\phi)$. From top to bottom, the blue lines correspond to $d(r_\phi)Q_\phi^2/C(r_\phi) = 1, 2, 4$. For red lines, this ordering is reversed. The dotted (dashed) lines give bounds from the total theoretical 1σ (2σ) uncertainties in the SM diphoton rate from VH production.

doublet, and triplet representations. Being color singlets, the scalars alter only the Higgs diphoton decay width. The crucial test here is to compare the branching ratios for the $\gamma\gamma$ and the VV^* channels, as deviation from the SM due to NP is expected in the diphoton width.

1. Singlets

We begin with singlets S without hypercharge. They are instrumental in constructing scalar dark matter models [11] and hidden or shadow Higgs models [12]. A gauge-invariant potential is given by

$$-\frac{\mu_1^2}{2}H^\dagger H+\frac{\lambda_1}{4}(H^\dagger H)^4-\frac{\mu_2^2}{2}S^\dagger S+\frac{\lambda_2}{4}(S^\dagger S)^2 + \frac{\lambda_3}{2}(S^\dagger S)(H^\dagger H). \tag{10}$$

If S does not undergo SSB, it will not mix with the SM doublet H, and will thus have no effect on the LHC signal.

The more interesting case is when both S and H undergo SSB. The mass matrix of the two scalars is not diagonal and is given by

$$\frac{1}{2}\begin{pmatrix}\lambda_1 v^2 & \lambda_3 v_s v\\ \lambda_3 v_s v & \lambda_2 v_s^2\end{pmatrix}, \tag{11}$$

where v_s (v) denotes the vacuum expectation value (VEV) of the singlet (doublet). Since S is an SM singlet, the Higgs coupling will receive in every vertex a universal suppression factor from the mixing angle that arises from diagonalizing the mass matrix above. This implies that $R_{\gamma\gamma}$ and R_{VV} would be suppressed by the same factor. An enhanced $R_{\gamma\gamma}$ would disfavor this case.

2. Doublets

As an archetypal example we consider here the two Higgs doublet model (2HDM). For simplicity we assume CP invariance. To avoid large flavor changing neutral currents, we assume also a discrete Z_2 symmetry such that only one of the Higgs doublets couples to u_R, and the other d_R and e_R. This is known as the type-II 2HDM. The Higgs sector of the minimal supersymmetric SM is a special case of this. A general review is given in Ref. [13].

The general gauge-invariant scalar potential in this model is given by

$$\begin{aligned}V(\Phi_1,\Phi_2) = &-\mu_1^2\Phi_1^\dagger\Phi_1-\mu_2^2\Phi_2^\dagger\Phi_2+\lambda_1(\Phi_1^\dagger\Phi_1)^2\\ &+\lambda_2(\Phi_2^\dagger\Phi_2)^2+\lambda_3(\Phi_1^\dagger\Phi_1)(\Phi_2^\dagger\Phi_2)\\ &-\lambda_4|\Phi_1^\dagger\Phi_2|^2-\frac{\lambda_5}{2}[(\Phi_1^\dagger\Phi_2)^2+(\Phi_2^\dagger\Phi_1)^2].\end{aligned} \tag{12}$$

Electroweak symmetry breaking is brought about by the VEV of Φ_i. Explicitly we write

$$\Phi_1=\begin{pmatrix}\phi_1^+\\ \frac{v_1+h_1+i\chi_1}{\sqrt{2}}\end{pmatrix},\qquad \Phi_2=\begin{pmatrix}\phi_2^+\\ \frac{v_2+h_2+i\chi_2}{\sqrt{2}}\end{pmatrix}. \tag{13}$$

The physics is best seen in the basis where only one of the doublets picks up a VEV:

$$\begin{pmatrix}\Phi_1'\\ \Phi_2'\end{pmatrix}=\begin{pmatrix}c_\beta & s_\beta\\ -s_\beta & c_\beta\end{pmatrix}\begin{pmatrix}\Phi_1\\ \Phi_2\end{pmatrix},\qquad \langle\Phi_1'\rangle=\begin{pmatrix}0\\ \frac{v}{\sqrt{2}}\end{pmatrix},\qquad \langle\Phi_2'\rangle=0. \tag{14}$$

We have used the shorthand notation $c_\theta=\cos\theta$, and we define $v^2=v_1^2+v_2^2$. The rotation angle is defined by $t_\beta\equiv\tan\beta=v_2/v_1$.

The physical degrees of freedom are projected out by a unitary gauge transformation:

$$\Phi_1'\to\begin{pmatrix}0\\ \frac{1}{\sqrt{2}}(v+\eta)\end{pmatrix},\qquad \Phi_2'\to\begin{pmatrix}H^+\\ \frac{1}{\sqrt{2}}(\phi+i\chi)\end{pmatrix}. \tag{15}$$

Here, η and ϕ are scalar fields, while χ is a pseudoscalar. The physical charged fields are the scalars $H^\pm$. This is not yet the mass eigenbasis. For the neutral scalars, the mass eigenbasis is given by

$$\begin{pmatrix}H^0\\ \Phi^0\end{pmatrix}=\begin{pmatrix}c_\alpha & s_\alpha\\ -s_\alpha & c_\alpha\end{pmatrix}\begin{pmatrix}\phi\\ \eta\end{pmatrix}. \tag{16}$$

We identify the lighter state, H^0, to be the candidate Higgs uncovered at the LHC. The mixing angle α is a complicated function of the parameters in the scalar potential, and the details are not needed here.

After some algebra the physical charged Higgs mass can be obtained from Eq. (12) and is given by

$$M_{H^\pm}^2\equiv\frac{1}{2}\bar\lambda v^2=\frac{1}{2}(\lambda_4+\lambda_5)v^2. \tag{17}$$

The triple scalar coupling $H^0H^+H^-$ can be also be worked out:

$$\begin{aligned}\lambda_{H^0H^+H^-}&\equiv\lambda_s M_W\\ &=v\left\{\left[\frac{1}{2}(\lambda_1+\lambda_2-\lambda_3+\bar\lambda)s_{2\beta}^2+\lambda_3\right]s_\alpha\right.\\ &\quad\left.-\left[\lambda_1 s_\beta^2-\lambda_2 c_\beta^2+\frac{1}{2}(\lambda_3-\bar\lambda)c_{2\beta}\right]s_{2\beta}c_\alpha\right\}.\end{aligned} \tag{18}$$

We see from above that the 2HDM is an example of non-decoupling scalars. If $M_{H^\pm}$ is taken large by taking $\bar\lambda$ large, $\lambda_{H^0H^+H^-}$ also becomes large. Requiring that the theory be perturbative, all couplings should be at least less than 4π, and $M_{H^\pm}$ cannot be much above the TeV scale.

Because of the scalar mixings, the couplings of the Higgs to fermions and gauge bosons are modified at the tree level. Thus σ_0 (in σ_{gg}) and $\Gamma_{\gamma\gamma}$ are modified in addition to the charged Higgs contribution entering at the one-loop level. In Table I, we list the modification to the relevant vertices. We also list their SM values for comparison. Note that we have

TABLE I. Triple vertices of the Higgs to fermions and gauge bosons in 2HDM and the SM.

Vertex	$H^0_{\rm 2HDM}$	$H^0_{\rm SM}$
$\bar{t}t$	$-ig_w \frac{M_t}{2M_w} \frac{\cos(\beta-\alpha)}{\sin\beta}$	$-ig_w \frac{M_t}{2M_W}$
$\bar{b}b$	$ig_w \frac{M_b}{2M_W} \frac{\sin(\beta-\alpha)}{\cos\beta}$	$-ig_w \frac{M_b}{2M_W}$
W^+W^-	$ig^{\mu\nu} g_w M_W \sin\alpha$	$ig^{\mu\nu} g_w M_W$
ZZ	$ig^{\mu\nu} g_w \frac{M_Z}{\cos\theta_w} \sin\alpha$	$ig^{\mu\nu} g \frac{M_Z}{\cos\theta_w}$

included the $H^0 b\bar{b}$ coupling because if t_β is large, the bottom contribution cannot be neglected.

With the modified couplings in hand, σ_0 in the GF production cross section is now

$$\sigma_0 = \frac{G_\mu \alpha_s^2}{128\sqrt{2}\pi} \left| \frac{1}{2}\left(\frac{c_\alpha}{t_\beta} + s_\alpha\right) F_{1/2}(\tau_t) - \frac{1}{2}(c_\alpha t_\beta - s_\alpha) F_{1/2}(\tau_b) \right|^2, \tag{19}$$

and the diphoton decay width is

$$\Gamma_{\gamma\gamma} = \frac{G_\mu \alpha^2 M_H^3}{128\sqrt{2}\pi^3} \left| s_\alpha F_1(\tau_W) + \frac{4}{3}\left(\frac{c_\alpha}{t_\beta} + s_\alpha\right) F_{1/2}(\tau_t) - \frac{1}{3}(c_\alpha t_\beta - s_\alpha) F_{1/2}(\tau_b) + \frac{\lambda_s}{\bar{\lambda}} F_0(\tau_{H^\pm}) \right|^2. \tag{20}$$

In deriving the above, we have expanded the trigonometric factors in terms of t_β, and we have used Eqs. (17) and (18).

Unlike the colored scalar case before, the Higgs decay widths can be quite different from the SM one. If $\beta \simeq \alpha$, the usual dominant $b\bar{b}$ decay channel can be suppressed by $\sin(\beta-\alpha)$. In this case the VV^* channel becomes dominant. Currently, this does not appear to be what is observed, although a firm conclusion is yet to be reached [4,5]. Assuming there are no accidental cancellations in the parameters, the $b\bar{b}$ and the VV widths are given by

$$\Gamma_{b\bar{b}} = (c_\alpha t_\beta - s_\alpha)^2 \Gamma^{\rm SM}_{b\bar{b}}, \qquad \Gamma_{VV} = s_\alpha^2 \Gamma^{\rm SM}_{VV}. \tag{21}$$

In Fig. 6 we show how $R_{\gamma\gamma}$ depends on the free parameters t_β, $\lambda_s/\bar{\lambda}$, and $M_{H^\pm}$. We see that there is little mass

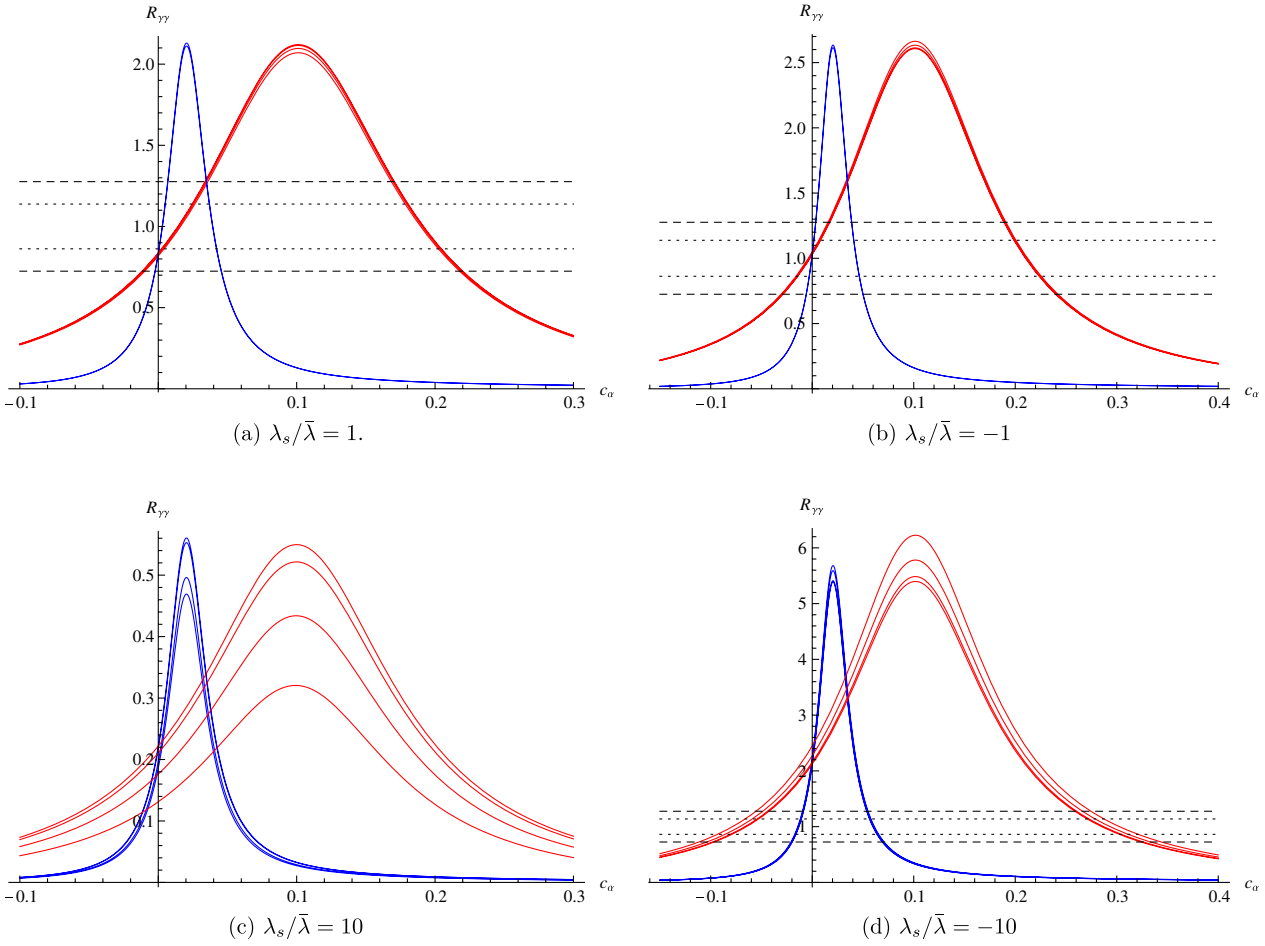

FIG. 6 (color online). The SM normalized production rate $R_{\gamma\gamma}$ for various values of $\tan\beta$, $\lambda_s/\bar{\lambda}$, and $M_{H^\pm}$. The red (blue, with peaks closer to the origin) lines correspond to $\tan\beta = 10(50)$. From bottom to top, the red lines correspond to $M_{H^\pm} = 109.6$, 150, 295, 2000 GeV, and the blue $M_{H^\pm} = 168.1$, 198.5, 548.1, 2000 GeV. The orderings reverse for negative values of $\lambda_s/\bar{\lambda}$. The dotted (dashed) lines give bounds from the total theoretical 1σ (2σ) uncertainties in the SM diphoton production rate.

dependence in general for $M_{H^\pm} > 500$ GeV, a manifestation of nondecoupling. The mass dependence also weakens as $\tan\beta$ increases, or as $\lambda_s/\bar{\lambda}$ decreases. In particular, for $\tan\beta = 50$ and $|\lambda_s/\bar{\lambda}| = 1$, $R_{\gamma\gamma}$ is virtually independent of $M_{H^\pm}$. For a given t_β the peak in $R_{\gamma\gamma}$ is also independent of $M_{H^\pm}$, as well as $\lambda_s/\bar{\lambda}$. The peak shifts towards smaller c_α as t_β increases. We see that for large $\lambda_s/\bar{\lambda}$, large enhancement in $R_{\gamma\gamma}$ can happen if it is negative, while suppression happens if it is positive.

Experimentally, the process $B^+ \to \tau^+\nu$ provides a stringent bound on $t_\beta/M_{H^\pm}$. Explicitly, we have [14]

$$r_b = \frac{\mathrm{BR}(B^+ \to \tau^+\nu)}{\mathrm{BR}_{\mathrm{SM}}(B^+ \to \tau^+\nu)} = \left(1 - \frac{m_{B^\pm}^2 t_\beta^2}{M_{H^\pm}^2}\right)^2. \quad (22)$$

Taking the average of the BELLE [15] and *BABAR* [16] results, the Heavy Flavor Averaging Group [17] finds the branching ratio $\mathrm{BR}(B^+ \to \tau^+\nu)$ to be $(1.64 \pm 0.34) \times 10^{-4}$. This implies that $r_b = 1.37 \pm 0.39$. Using this at the 95% confidence level, $M_{H^\pm} > 109.6$ GeV is allowed at $t_\beta = 10$, while at $\tan\beta = 50$, $M_{H^\pm}$ is allowed between 168.1 and 198.5 GeV, and also above 548.1 GeV.

For type-II 2HDM, there is actually a t_β-independent bound of $M_{H^\pm} > 295$ GeV coming from the inclusive $b \to s\gamma$ decay [18]. However, this assumes that the only NP contribution comes from the 2HDM and nothing else. Applying this bound would mean that in Fig. 6 the lower (top) two red and blue curves in plots with positive (negative) $\lambda_s/\bar{\lambda}$ are ruled out.

In Fig. 7 we show how R_{VV} depends on the free parameters t_β, $\lambda_s/\bar{\lambda}$, and $M_{H^\pm}$. The total theoretical 1σ uncertainties in the SM Higgs VV^* production rate is $\pm 13.4\%$. We see that R_{VV} is practically independent of $M_{H^\pm}$. This is because the mass dependence enters only in $\Gamma_{\gamma\gamma}$ and is weak. Moreover, the branching ratio to two photons is small compared with the other channels. Thus the total width and hence R_{VV} hardly varies with $M_{H^\pm}$. For the same reason, there is also little dependence on $\lambda_s/\bar{\lambda}$, which again enters only in $\Gamma_{\gamma\gamma}$.

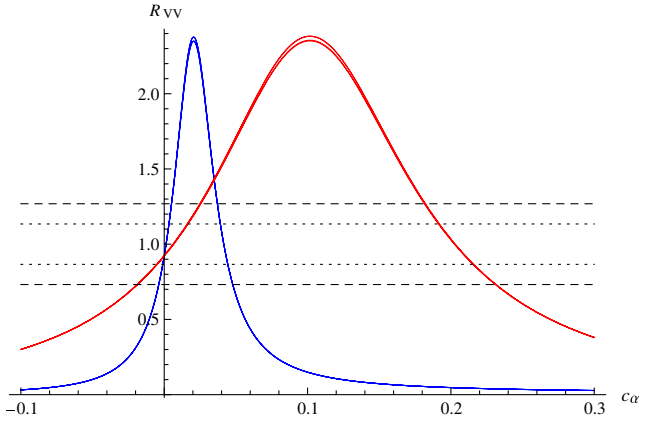

FIG. 7 (color online). The SM normalized production rate R_{VV} for various values of $\tan\beta$ and $\lambda_s/\bar{\lambda}$. The red (blue, with peaks closer to the origin) lines correspond to $\tan\beta = 10(50)$. The bottom (top) lines correspond to $\lambda_s/\bar{\lambda} = -10(10)$. The dotted (dashed) lines give bounds from the total theoretical 1σ (2σ) uncertainties in the SM Higgs VV^* production rate.

Comparing Figs. 6 and 7, for a given t_β, R_{VV} is quite different from $R_{\gamma\gamma}$ for large $\lambda_s/\bar{\lambda}$, but comparable for small $\lambda_s/\bar{\lambda}$ ($|\lambda_s/\bar{\lambda}| \lesssim 1$). Thus a comparison between R_{VV} and $R_{\gamma\gamma}$ may in addition be used to gauge the magnitude of $\lambda_s/\bar{\lambda}$.

3. Triplets

Besides being of interest in their own rights, models incorporating both a doublet and a triplet Higgs fields are common in models of neutrino masses from type-II seesaw mechanism [19] and quantum radiative corrections [20].

We consider here the simple case where the Higgs triplet carries no hypercharge ($Y = 0$). The Higgs doublet and triplet fields are respectively given by

$$H = \begin{pmatrix} h^+ \\ \frac{1}{\sqrt{2}}(v_h + h^0 + i\chi) \end{pmatrix}, \qquad T = \begin{pmatrix} \frac{1}{2}(v_T + T^0) & \frac{1}{\sqrt{2}}T^+ \\ \frac{1}{\sqrt{2}}T^- & -\frac{1}{2} - (v_T + T^0) \end{pmatrix}, \quad (23)$$

where v_h (v_T) denotes the VEV of the H (T) field. For clarity, we have changed slightly the notation for the Higgs doublet from the previous subsection.

The most general, gauge-invariant and renormalizable potential is given by

$$V(H,T) = -\mu_H^2 H^\dagger H + \frac{\lambda_H}{4}(H^\dagger H)^2 - \mu_T^2 \mathrm{Tr}T^2 + \frac{\lambda_T}{4}(\mathrm{Tr}T^2)^2 + \kappa H^\dagger H \mathrm{Tr}T^2 + \mu H^\dagger T H. \quad (24)$$

The physical spectrum consists of pairs of neutral and charged scalars. An important feature here is that v_T contributes to the W boson mass, whereas the Z boson mass comes only from v_h. This gives rise to a tree-level correction to the ρ parameter:

$$\rho = 1 + 4\frac{v_T^2}{v_h^2}. \quad (25)$$

A global fit of the electroweak precision data gives $\rho = 1.0008^{+.0017}_{-.0007}$ [21], from which we obtain the bound $v_T < 4$ GeV.

Parameters of the potential $V(H,T)$ are not all independent. Minimizing the potential, we have the relations

$$\mu_H^2 - \frac{1}{4}\lambda_H v_h^2 - \frac{1}{2}\kappa v_T^2 + \frac{1}{2}\mu v_T = 0, \quad (26)$$

$$\left(\mu_T^2 - \frac{1}{4}\lambda_T v_T^2 - \frac{1}{2}\kappa v_h^2\right)v_T + \frac{1}{4}\mu v_h^2 = 0. \quad (27)$$

With v_h and v_T being the input parameters and nonzero, these imply

$$\kappa = \frac{4\mu_T^2 - \lambda_T v_T^2}{v_h^2} - \frac{4\mu_H^2 - \lambda_H v_h^2}{2v_T^2},$$
$$\mu = \frac{v_T(4\mu_T^2 - \lambda_T v_T^2)}{v_h^2} - \frac{4\mu_H^2 - \lambda_H v_h^2}{v_T}. \quad (28)$$

Note that in the exact limit where $v_T = 0$, we can only minimize the potential with respect to H, and we get the usual condition $2\mu_H = v_h\sqrt{\lambda_H}$.

Consider now the charged states. From Eq. (24), their mass matrix is given by

$$M_\pm^2 = \begin{pmatrix} \mu v_T & \frac{1}{2}\mu v_H \\ \frac{1}{2}\mu v_H & \frac{\mu v_H^2}{4v_T} \end{pmatrix}. \quad (29)$$

Diagonalizing and using the physical charged mass eigenstates given by

$$\begin{pmatrix} H^\pm \\ G^\pm \end{pmatrix} = \begin{pmatrix} c_\theta & s_\theta \\ -s_\theta & c_\theta \end{pmatrix}\begin{pmatrix} T^\pm \\ h^\pm \end{pmatrix}, \quad (30)$$

where the mixing angle is defined by

$$c_\theta = \frac{v_h}{v}, \qquad s_\theta = 2\frac{v_T}{v}, \qquad v^2 = v_h^2 + 4v_T^2, \quad (31)$$

$G^\pm$ are massless would-be-Goldstone bosons, and $H^\pm$ the physical charged Higgs with mass given by

$$M_{H^\pm}^2 = \mu v_T\left(1 + \frac{v_h^2}{4v_T^2}\right)$$
$$= (4\mu_T^2 - \lambda_T v_T^2)\left(\frac{1}{4} + \frac{v_T^2}{v_h^2}\right) - (4\mu_H^2 - \lambda_H v_h^2)\left(1 + \frac{v_h^2}{4v_T^2}\right), \quad (32)$$

after using Eq. (28). We see that since $t_\theta \equiv \tan\theta = 2(v_T/v_h)$ is small, $H^\pm$ are mostly composed of $T^\pm$.

From Eq. (32), the physical charged Higgs mass would be naturally in the TeV range. If we take the limit $t_\theta \ll 1$ while keeping all other independent parameters ($\mu_{H,T}$ and $\lambda_{H,T}$) fixed, $H^\pm$ would become very heavy and thus decouple. However, if in addition we take $4\mu_H^2 - \lambda_H v_h^2 = -k^2 v_T^2$ for some fixed k, then $M_{H^\pm} = \frac{v}{2}\sqrt{\kappa + \frac{k^2}{2}}$ can remain at the weak scale, and $H^\pm$ would not decouple. We note here that although the two cases have different theoretical implications, the Higgs signal itself would not be able to distinguish between the two.

Consider next the neutral states, whose mass matrix is given by

$$M_0^2 = \begin{pmatrix} \frac{1}{2}\lambda_H v_h^2 & \left(\kappa v_T - \frac{1}{2}\mu\right)v_h \\ \left(\kappa v_T - \frac{1}{2}\mu\right)v_h & \frac{1}{2}\lambda_T v_T^2 + \frac{\mu v_h^2}{4v_T} \end{pmatrix}, \quad (33)$$

and the mass eigenbasis

$$\begin{pmatrix} H^0 \\ \Phi^0 \end{pmatrix} = \begin{pmatrix} c_\xi & s_\xi \\ -s_\xi & c_\xi \end{pmatrix}\begin{pmatrix} h^0 \\ T^0 \end{pmatrix}. \quad (34)$$

The mass eigenvalues are given by

$$M_{H^0,\Phi^0}^2 = \frac{1}{8}(A \mp \sqrt{A^2 + 4B^2 t_\theta^2}), \quad (35)$$

where

$$A = 2(\lambda_H + \kappa)v_h^2 + 3\lambda_T v_T^2 - 4\mu_T^2,$$
$$B = \lambda_T v_T^2 - 4\mu_T^2. \quad (36)$$

We take H^0 to be the lighter state and thus with the negative sign. Expanding in small t_θ up to $\mathcal{O}(t_\theta^3)$, the masses are given by

$$M_{H^0}^2 = \frac{1}{2}\lambda_H v_h^2 - \frac{B^2 t_\theta^2}{4A},$$
$$M_{\Phi^0}^2 = \frac{1}{4}(2\kappa v_h^2 + 3\lambda_T v_T^2 - 4\mu_T^2) + \frac{B^2 t_\theta^2}{4A}, \quad (37)$$

and the mixing

$$c_\xi = 1 - \frac{B^2}{2A^2}t_\theta^2, \qquad s_\xi = \frac{B}{A}t_\theta. \quad (38)$$

We see from this that H^0 is SM-like (mostly doublet), and we identify it as the LHC Higgs candidate.

We can now work out the cubic couplings of H^0 that contribute to its production and decay. The scalar coupling $H^0H^+H^-$ comes from the vertex $h^0T^+T^-$ in the gauge basis, and is given by $c_\theta^2 c_\xi \kappa v_h$. Since the triplet does not contribute to fermion mass generation, the $H^0 f\bar{f}$ Yukawa coupling is just the SM one with an additional c_ξ factor. For the H^0 coupling to gauge bosons, both the doublet and the triplet contribute. But since the former $\sim v_h$ while the latter $\sim v_T$, the triplet contribution can be neglected in comparison to the doublet. Thus, the H^0 coupling to gauge bosons is again just the SM one with an extra c_ξ factor. However, this factor cancels out in the production rate between the production cross section and the branching ratios. Thus, when calculating production rates, the modification from the SM come only from the charged Higgs contribution to $\Gamma_{\gamma\gamma}$.

Working in the small t_θ limit with $(4\mu_H^2 - \lambda_H v_h^2)/v_T^2 = -k^2$ fixed, the $H^0H^+H^-$ coupling is simply

$$\lambda_{H^0H^+H^-} = \kappa v = \frac{4M_{H^\pm}^2}{v}\left(1 - \frac{k^2 v^2}{8M_{H^\pm}^2}\right). \quad (39)$$

It is convenient to redefine the coupling with $M_{H^\pm}^2$ scaled out, i.e. we define

$$\lambda_{H^0H^+H^-} M_W = \lambda g_w M_{H^\pm}^2. \quad (40)$$

The Higgs diphoton decay width is then

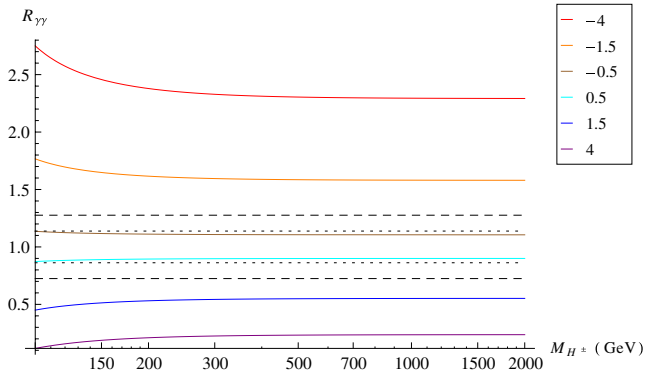

FIG. 8 (color online). The SM normalized production rate $R_{\gamma\gamma}$ for various values of λ as denoted by the colored lines. [From top to bottom, the lines correspond to $\lambda = -4$ to 4.] The dotted (dashed) lines give bounds from the total theoretical 1σ (2σ) uncertainties in the SM diphoton production rate.

$$\Gamma_{\gamma\gamma} = \frac{G_\mu \alpha^2 M_H^3}{128\sqrt{2}\pi^3} \left| F_1(\tau_W) + \frac{4}{3} F_{1/2}(\tau_t) + \lambda F_0(\tau_{H^\pm}) \right|^2, \tag{41}$$

and we see clearly that the charged Higgs do not decouple.

We show in Fig. 8 the behavior of $R_{\gamma\gamma}$ as a function of $M_{H^\pm}$ for various values of λ. We see that the nondecoupling behavior sets in very quickly at about 300 GeV. Enhancement in $R_{\gamma\gamma}$ happens for negative values of λ. Neglecting the effects of mixing which are small, the predictions here are that $R_{\gamma\gamma} = R_{\gamma\gamma}^{VH} \neq 1$ and $R_{VV} = 1$.

IV. CONCLUSIONS

In this work, we have examined the constraints on scalar NP from the recent LHC Higgs signals. We have studied in detail how parameters relating to different new scalars can be constrained in a general way by using $R_{\gamma\gamma}$, R_{VV} and $R_{\gamma\gamma}^{VH}$ in conjunction with each other. If the trend of the current data persists, these constraints can be used to aid the detection of new scalar states at the LHC, and even to distinguish them. Indeed, the example of the Higgs triplet has shown that its existence can be revealed by having measured $R_{\gamma\gamma} = R_{\gamma\gamma}^{VH} \neq 1$ and $R_{VV} = 1$, independent of what other roles it may play. Thus, the importance of measuring R_{VV} and $R_{\gamma\gamma}^{VH}$ in addition to $R_{\gamma\gamma}$ cannot be overemphasized.

In general, if the mass generation mechanism of a new state is not related to the electroweak symmetry breaking scale, decoupling occurs. Examples we have given are colored scalars, with or without electric charge. Their effect on the Higgs signal drop away as they become heavier and heavier. For scalars from an extended Higgs sector where mixings occur, this does not hold in general. This has been illustrated in detail in our study of the type-II 2HDM and the $Y = 0$ triplet model. The SM normalized production rates such as $R_{\gamma\gamma}$ would asymptote to constant values different from unity in the large mass limit, and these would give a measure of the effective triple scalar coupling. Of course, nondecoupling behavior is already seen in fourth generation studies. It is well known that fourth generation fermion masses are proportional to their Yukawa couplings, and so they are nondecoupling in our classification. Because of this, even with the currently very limited statistics, a simple fourth generation extension of the SM appears untenable [22].

We have paid special attention to the type-II 2HDM because it is archetypal in many theoretical and phenomenological constructions. We have shown that by including constraints from B meson decays, the Higgs signal can be used to probe the neutral scalar mixings, which is a general feature of the model. For enhancement in $R_{\gamma\gamma}$, small values of c_α are preferred in general. For large $\tan\beta$, $R_{\gamma\gamma}$ is insensitive to the mass of the charged Higgs. For smaller values of $\tan\beta$, there is more sensitivity to the other parameters.

As in all indirect searches of NP, it is possible that more than one species of the new degrees of freedom can enter into the observables, and accidental cancellations can happen to negate the constraints found for a single species. This is a caveat we have to bear in mind.

ACKNOWLEDGMENTS

W.-F. C. is supported by the Taiwan NSC, Grant No. 99-2112-M-007-006-MY3. J. N. N. is partially supported by Natural Science and Engineering Council of Canada. J. M. S. W. is supported by NCTS.

[1] Atlas Collaboration, Report No. ATLAS-CONF-2012-019; CMS Collaboration, Report No. CMS-PAS-HIG-12-008.
[2] G. Aad *et al.* (ATLAS Collaboration), Phys. Rev. Lett. **108**, 111803 (2012).
[3] S. Chatrchyan *et al.* (CMS Collaboration), Phys. Lett. B **710**, 403 (2012).
[4] G. Aad *et al.* (ATLAS Collaboration), Phys. Lett. B **710**, 383 (2012).
[5] S. Chatrchyan *et al.* (CMS Collaboration), Phys. Rev. Lett. **108**, 111804 (2012).
[6] TEVNPH (Tevatron New Phenomena and Higgs Working Group and CDF and D0 Collaborations), arXiv:1203.3774.

[7] R. Bonciani, G. Degrassi, and A. Vicini, J. High Energy Phys. 11 (2007) 095; G. Cacciapaglia, A. Deandrea, and J. Llodra-Perez, J. High Energy Phys. 06 (2009) 054; A. Azatov, M. Toharia, and L. Zhu, Phys. Rev. D **82**, 056004 (2010); J. Cao, Z. Heng, T. Liu, and J. M. Yang, Phys. Lett. B **703**, 462 (2011); Y. Bai, J. Fan, and J. L. Hewett, arXiv:1112.1964; B. A. Dobrescu, G. D. Kribs, and A. Martin, Phys. Rev. D **85**, 074031 (2012); U. Ellwanger, J. High Energy Phys. 03 (2012) 044; B. Batell, S. Gori, and L.-T. Wang, J. High Energy Phys. 06 (2012) 172; G. Belanger, A. Belyaev, M. Brown, M. Kakizaki, and A. Pukhov, Eur. Phys. J. Web Conf. **28**, 12070 (2012); V. Barger, M. Ishida, and W.-Y. Keung, Phys. Rev. Lett. **108**, 261801 (2012); M. Carena, S. Casagrande, F. Goertz, U. Haisch, and M. Neubert, arXiv:1204.0008; P. Draper and D. McKeen, Phys. Rev. D **85**, 115023 (2012); K. Kumar, R. Vega-Morales, and F. Yu, arXiv:1205.4244; S. Dawson and E. Furlan, arXiv:1205.4733 [Phys. Rev. D (to be published)]; M. Carena, S. Gori, N. R. Shah, C. E. M. Wagner, and L.-T. Wang, arXiv:1205.5842; A. G. Akeroyd and S. Moretti, arXiv:1206.0535; M. Carena, I. Low, and C. E. M. Wagner, arXiv:1206.1082; L. Wang and X.-F. Han, arXiv:1206.1673; V. Illisie and A. Pich, arXiv:1202.3420.

[8] A. Djouadi, Phys. Rep. **457**, 1 (2008).

[9] CMS Collaboration, Report No. CMS PAS HIG-12-008.

[10] https://twiki.cern.ch/twiki/bin/view/LHCPhysics/CrossSections.

[11] C. A. de S. Pires, F. S. Queiroz, and P. S. Rodrigues da Silva, Phys. Rev. D **82**, 105014 (2010); C. Englert, T. Plehn, M. Rauch, D. Zerwas, and P. M. Zerwas, Phys. Lett. B **707**, 512 (2012).

[12] W.-F. Chang, J. N. Ng, and J. M. S. Wu, Phys. Rev. D **75**, 115016 (2007).

[13] G. C. Branco, P. M. Ferreira, L. Lavoura, M. N. Rebelo, M. Sher, and J. P. Silva, Phys. Rep. **516**, 1 (2012).

[14] W. S. Hou, Phys. Rev. D **48**, 2342 (1993); Y. Grossman and Z. Ligeti, Phys. Lett. B **332**, 373 (1994).

[15] K. Ikado *et al.* (Belle Collaboration), Phys. Rev. Lett. **97**, 251802 (2006).

[16] B. Aubert *et al.* (*BABAR* Collaboration), Phys. Rev. D **81**, 051101 (2010).

[17] http://www.slac.stanford.edu/xorg/hfag.

[18] M. Rozanska, Proc. Sci., CHARGED2010 (2010) 005.

[19] G. Passrino, Phys. Lett. B **231**, 458 (1989); M. C. Chen, S. Dawson, and T. Krupovnickas, Phys. Rev. D **74**, 035001 (2006).

[20] C. S. Chen, C. Q. Geng, J. N. Ng, and J. M. S. Wu, J. High Energy Phys. 08 (2007) 022.

[21] K. Nakamura *et al.* (Particle Data Group), J. Phys. G **37**, 075021 (2010), and 2011 partial update for the 2012 edition.

[22] A. Djouadi and A. Lenz, arXiv:1204.1252; E. Kuflik, Y. Nir, and T. Volansky, arXiv:1204.1975.